analytical chemistry

TECHNICAL NOTE

pubs.acs.org/ac

Multifunctional Picoliter Droplet Manipulation Platform and Its Application in Single Cell Analysis

Shu-Qing Gu, Yun-Xia Zhang, Ying Zhu, Wen-Bin Du,† Bo Yao, and Qun Fang*

Department of Chemistry, Institute of Microanalytical Systems, Zhejiang University, Hangzhou 310058, China

Supporting Information

ABSTRACT: We developed an automated and multifunctional microfluidic platform based on DropLab to perform flexible generation and complex manipulations of picoliter-scale droplets. Multiple manipulations including precise droplet generation, sequential reagent merging, and multistep solid-phase extraction for picoliter-scale droplets could be achieved in the present platform. The system precision in generating picoliter-scale droplets was significantly improved by minimizing the thermo-induced fluctuation of flow rate. A novel droplet fusion technique based on the difference of droplet interfacial tensions was developed without the need of special microchannel networks or external devices. It enabled sequential addition of reagents to droplets on demand for multistep reactions. We also developed an effective picoliter-scale droplet splitting technique with magnetic actuation. The difficulty in phase separation of magnetic beads from picoliter-scale droplets due to the high interfacial tension was overcome using ferromagnetic particles to carry the magnetic beads to pass through the phase interface. With this technique, multistep solid-phase extraction was achieved among picoliter-scale droplets. The present platform had the ability to perform complex multistep manipulations to picoliter-scale droplets, which is particularly required for single cell analysis. Its utility and potentials in single cell analysis were preliminarily demonstrated in achieving high-efficiency single-cell encapsulation, enzyme activity assay at the single cell level, and especially, single cell DNA purification based on solid-phase extraction.

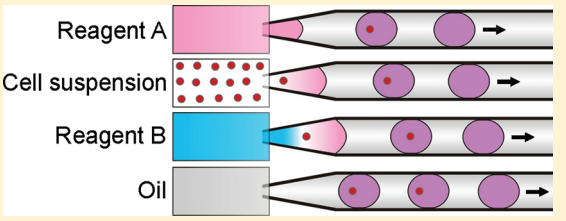

Droplet-based microfluidics offers an attractive platform for performing chemical and biological reactions due to its abilities of eliminating diffusion and accelerating mass transfer.[1−3] Various microfluidic techniques for droplet generating,[4,5] mixing,[6,7] fusion,[8−10] and splitting[11,12] have been developed and applied in reaction kinetics studies,[6] protein crystallization,[7] chemical synthesis,[8,10] and nucleic acid assays.[13,14] Currently, most of the reported droplet systems are built under continuous flow mode,[4−8,10−14] which have advantages of high throughput in droplet generation and analysis, as well as small droplet volumes in the range of nanoliters to picoliters or even femtoliters. However, performing complex and multistep droplet manipulations usually presents challenges in these systems. For droplet systems working under batch mode, such as digital microfluidic[15,16] and magnetic-actuated droplet[17,18] systems, although their analysis throughputs are relatively lower than the former ones, they can flexibly perform various droplet manipulations to achieve cell assays,[15] proteomic sample processing,[16] and nucleic acid-based assays[17,18] with complicated operations. In these systems, the volumes of the manipulated droplets are usually in the range of microliters to nanoliters.[15−18] Despite the great success of droplet-based systems, multifunctional microfluidic platforms that can perform complex and multiple manipulations for picoliter-scale droplets including droplet generation, transport, combining, and splitting are still scarce.

Droplet-based microfluidic systems with droplet volumes in the picoliter range particularly provide an ideal platform for single cell analysis for eliminating sample dilution and cross-contamination.[3,19] Various droplet systems have been reported to achieve cell encapsulation,[20] culture,[21] sorting,[22] enzyme assay,[23,24] protein expression,[24,25] and measurement of low abundance of surface biomarkers[26] at the single cell level. In spite of these successful applications, a multifunctional droplet platform capable of performing complex operations for single cell analysis still presents challenges. For example, the solid-phase extraction of nucleic acids from a single cell, which had been achieved using PDMS chip with multiple pneumatic microvalves,[27,28] has still not been realized in the droplet-based system. Moreover, microfluidic systems based on magnetic actuation[15,16] or digital microfluidics[17,18] capable of performing complicated droplet manipulations have not yet been applied in single cell analysis, probably due to the relatively large droplet volumes.

In 2010, we developed DropLab,[29] an automated microfluidic system for droplet-based assay and screening based on the droplet assembling technique, which has high controllability on the compositions and volumes of droplets in the nanoliter to picoliter range. This system was applied in enzyme inhibition

Received: June 30, 2011
Accepted: August 25, 2011
Published: August 25, 2011

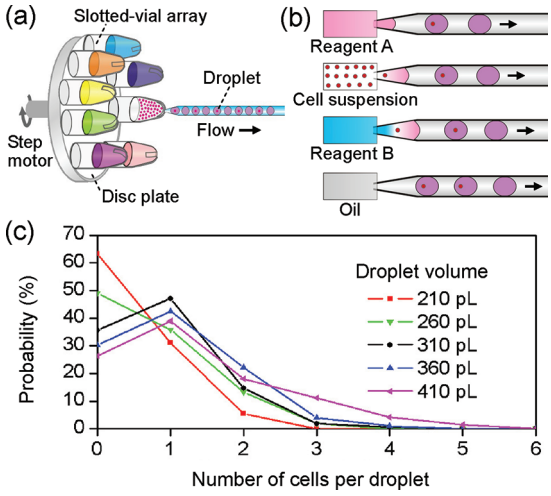

Figure 1. (a) Setup of the DropLab platform (not to scale). (b) Schematic diagram of principle for encapsulation of single cells. (c) The probability distribution of different cell number per droplet with different droplet volumes. Each curve was counted from data of 300 droplets using the suspensions with the same cell density (3.25×10^6 cells/mL).

assay and protein crystallization screening. In this work, we improved the system precision for generating picoliter-scale droplets and developed two novel techniques for complex picoliter-scale droplet manipulations, including sequential droplet fusion based on interfacial tension difference of droplets and multistep solid-phase extraction based on magnetic-assisted picoliter-scale droplet splitting. On the basis of these techniques, we built a multifunctional droplet-based microfluidic platform capable of performing complex multistep manipulations for picoliter-scale droplets. Picoliter-scale droplets in particular offer an attractive tool for single cell analysis, as the confined volumes defined by the droplet can prevent dilution of the low copy number of proteins and molecules in such biological samples. We applied the present platform in single cell analysis and preliminarily demonstrated its utility and potentials in this area in achieving high probability encapsulation for single cell, single cell enzyme activity assay, and single cell DNA purification based on solid-phase extraction.

EXPERIMENTAL SECTION

The setup of the droplet-based single cell analysis platform was similar to DropLab described previously.[18] Briefly, it consisted of a 5 cm long fused-silica capillary (75 μm i.d., 375 μm o.d., Reafine Chromatography Co., Yongnian, China) with a tapered tip (tip diameter, 25 μm), a picoliter precision syringe pump (Harvard Apparatus, Holliston, MA), and a slotted-vials array (SVA) liquid-presenting system (Figure 1a). The operations of the SVA system and syringe pump were under control of a program written in LabVIEW.

Before use, the tip and channel walls of the tapered capillary were silanized to obtain a hydrophobic surface. The slotted vials were filled with 5−10 μL of cell suspensions, reagents, and oil. Under control of the program, the SVA was rotated to allow the capillary tip to sequentially enter the liquids filled in different vials through the slots, aspirating definite volumes of the liquids into the capillary to generate a series of aqueous droplets for single cell analysis under the droplet assembling mode (Figure 1b). The detailed description of the experimental section is provided in the Supporting Information.

RESULTS AND DISCUSSION

Improvement of Precision for Generating Picoliter Droplets. Precise control to droplet volumes is a prerequisite for a droplet-based platform. The control difficulty increases with the decrease of droplet volumes, especially for picoliter-scale droplets. In the present system, since the droplet assembling method was used to generate droplets, the precision of aspirating flow rate of the syringe pump had a significant influence on the precision of droplet volumes. In the preliminary experiments for continuously generating 300 pL droplets, we observed an evident fluctuation of the liquid flow rate in the capillary channel, which resulted in a variation range of 200−400 pL and a RSD of 12.4% (n = 100) for droplet sizes (Figure S1a, Supporting Information). This fluctuation of flow rate was caused by the repeated expansion and shrinkage of the oil filled in the syringe with the variation of the ambient temperature. The expansion and shrinkage of oil still existed even when the syringe pump was stopped, which was shown as a position fluctuation of the droplets formed in the capillary. We investigated the relationship between the variations of the ambient temperature and the position of a droplet in the capillary at stopped-flow condition and found that their variation tendencies were consistent (as shown in Figure S2, Supporting Information). In order to minimize this thermo-induced fluctuation of flow rate, we used an adiabatic shield for the syringe and capillary to protect them from ambient temperature variation. The precision of droplet sizes was improved to 7.7% (RSD, n = 50). For further reducing this thermal effect, we filled water in the syringe instead of the oil, since the thermal expansion coefficient of water (2.5×10^{-4}/°C, 25 °C) is much smaller than the oil (8.7×10^{-4}/°C, 25 °C). As a result, the variation range and RSD of the droplet sizes were improved to 280−320 pL and 2.8% (n = 100), respectively (Figure S1b, Supporting Information). Such a precision of droplet sizes is comparable to those (1.7%−5.0%, RSD) previously reported in droplet systems under continuous-flow mode for single cell analysis.[20,21,25] If needed, the precision could be further improved using a syringe pump with higher precision or a gastight syringe with less volume or installing the whole setup in a thermostat cover.

Application in Single Cell Enzyme Assay. With the improvement in volume precision of picoliter droplets, we first applied the system in single cell enzyme assay to demonstrate its feasibility, in which single-cell encapsulation and multiple reagent addition are required to perform in picoliter droplets. The single-cell encapsulation was carried out using the bulk average approach. The single cell droplets were formed using droplet assembling mode by sequentially aspirating cell suspension, reagent solutions, and oil carrier into the capillary (Figure 1b). The stable aspirating flow rate enabled the system to flexibly and accurately adjust the volume of the cell suspension introduced into the droplets with a 20 pL minimum unit, to ensure the highest single cell encapsulation efficiency. We investigated the distribution of cell number per droplet in the cell encapsulation experiment using a rat pheochromocytoma (PC12) cell suspension (3.25×10^6 cells/mL) as the sample with different droplet volumes in the range of 210−410 pL. As shown in Figure 1c, the cell distribution for each droplet volume showed good agreement with Poisson distribution.[20] A highest efficiency of 47% for single cell encapsulation was obtained with a 310 pL droplet volume,

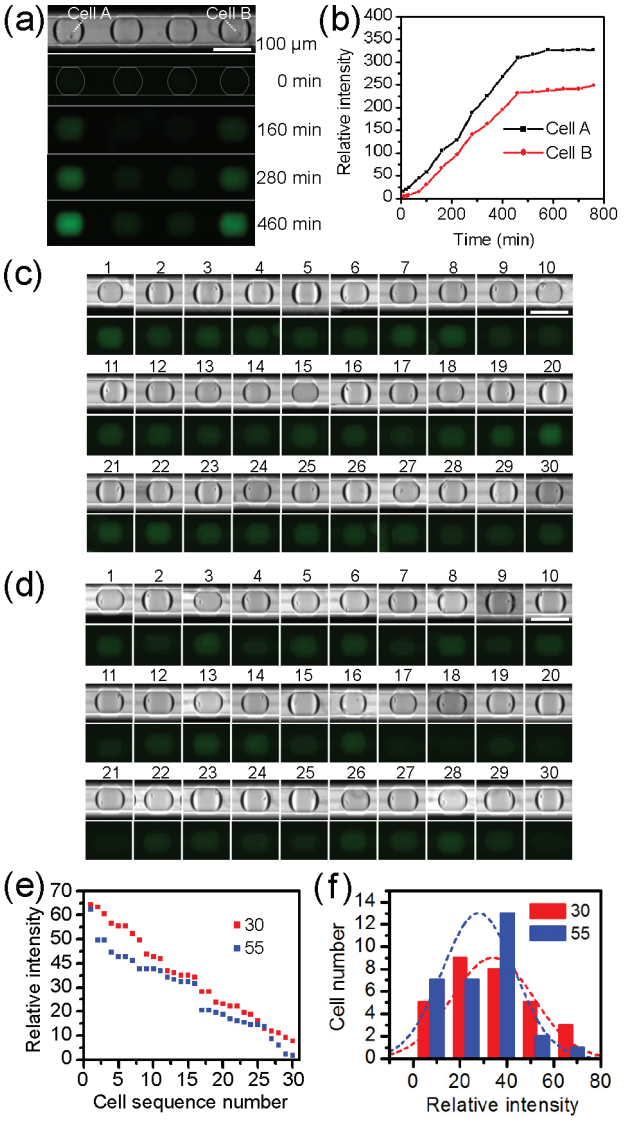

Figure 2. (a) Bright-field image of a four-droplet array with two single-cell droplets and two blank droplets, and fluorescence images of the droplet array at different reaction times during the intracellular enzyme activity assay. (b) Time-intensity curves of the two single-cell droplets in (a) within a 12 h period. (c) and (d) Bright-field and fluorescence images of 30 droplets containing single PC12 cells of (c) passage 30 and (d) passage 55. (e) List of the droplet fluorescence intensities in descending order in (c) and (d), respectively. (f) Histograms of normal distributions of the cell number at different fluorescence intensity regions in (c) and (d) with Gaussian fits, respectively. The divided fluorescence intensity regions were 0−15, 15−30, 30−45, 45−60, and 60−75 relative intensity. Scale bar: 100 μm.

which is approximately 10% higher than the values reported by other groups.[21,24] This may be caused by the rotation of the SVA system which shook the cell suspension in the vial and avoided the settlement and aggregation of cells as usually occurs in microfabricated devices. Without the precision improvement in droplet volumes, the encapsulation efficiency for single cells was approximately 27%. The high controllability on droplet volumes could enable the present platform to flexibly meet different requirements in single cell analysis, such as high single-cell occupancy in all droplets,[22] compromise between single-cell encapsulation efficiency and cell utilization,[20] or assured single-cell occupancy in cell-containing droplets.[26]

The PC12 cells were used as model samples to perform the intracellular enzyme activity assay of β-galactosidase at single-cell level. A series of 300 pL droplets composed of a 100 pL cell suspension; 100 pL, 200 μM substrate fluorescein di-β-D-galacto-pyranoside (FDG) solution; and 100 pL 0.2% Triton X-100 solution for cell lysis was generated in the capillary channel. Within the picoliter-droplet reactors, the cells were lysed and released intracellular enzymes including β-galactosidase. The substrate FDG in droplet was converted by β-galactosidase to fluorescein monogalactoside and fluorescein which was detected by the fluorescence microscope. The cell lysis process was achieved in 30−120 s. We performed a 12 h long-time monitoring of the fluorescence intensities of two typical single-cell droplets to obtain a profile of the whole enzyme-catalyzed reaction process within droplets. The results are shown in Figure 2a,b. The fluorescence intensities of the two droplets without cells which could be used as blank droplets were also monitored simultaneously with the two single cell droplets. The fluorescence signals of the blank droplets showed a slight increase with the time (as shown in Figure S3, Supporting Information) which was probably caused by the autohydrolysis of the substrate. In the single cell enzyme assay, the average fluorescence signal of the blank droplets was deducted as background from those of the single cell droplets (Figure 2a,b). The fluorescence intensities of the two single cell droplets showed similar trends of significant increase with the time within the first 7 h and tended to level off in 7−12 h which was possibly caused by the inactivation of the enzyme. The difference between the two signal values at the same time points may be attributed to the individual cell variation. These results indicate that it is possible to measure the activities of low-abundance enzymes in single cells by detecting their catalytic products accumulated in the picoliter droplets during a long reaction period.

One of the features of the present platform lies in the ability in generating droplets with different compositions; thus, it is possible to apply it in simultaneous analysis for different cell samples. To demonstrate this feasibility, we used the platform to measure the intracellular β-galactosidase activity of PC12 cells at different passages simultaneously. The droplets containing single PC12 cells at 30 and 55 passages were generated alternatively, and their fluorescence intensities were measured after a 100 min incubation. The results of 60 cells at the two passages are shown in Figure 2c−f. Figure 2e shows a list of the droplet fluorescence intensities for the two different cell samples in descending order. Figure 2f shows the histograms of normal distributions of the data shown in Figure 2e, which were yielded by dividing the fluorescence intensity range into five regions. The intracellular β-galactosidase activity of the PC12 cells at the same age exhibited a large degree of heterogeneity due to individual difference, and the distribution of single-cell enzyme activities at different passages showed slight difference.

Sequential Droplet Fusions Based on Interfacial Tension Difference. For multistep biochemical reactions, including those involved in complex single cell analysis, some reagents are required to be added to the formed droplets at defined times during the reaction period. This can be achieved by inducing the fusion of droplets in microfluidic networks using various manipulation means based on electrostatics, optics, and specific channel geometry.[8−10] However, these manipulations for droplet fusion are difficult to perform in a capillary-based system.

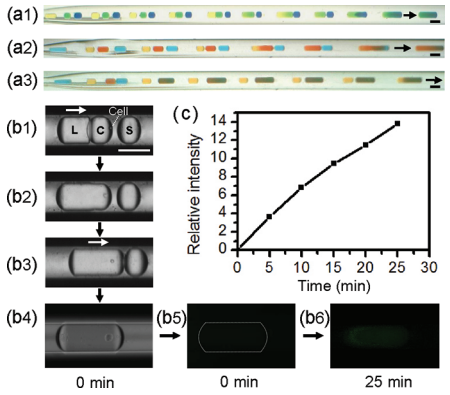

Figure 3. (a1) and (a2) Sequential fusion in multiple droplet groups. Each group consists of three droplets containing different dye solutions. (a3) Changing fusion sequence in (a2) by adjusting the oil volume between the three droplets. (b1−b6) Single cell enzyme assay by sequential fusion of 500 pL of cell lysis buffer droplet (L), 250 pL of single cell droplet (C), and 250 pL of enzyme substrate droplet (S). (b1) Cell lysis buffer droplet (PBS solution containing 0.2% Triton X-100 and 0.2% Tween 20) fuses with single cell droplet; (b2) The cell is lysed in the droplet within 5 min; (b3) Enzyme substrate droplet fuses with the cell-lysed droplet; (b4) Bright-field image of the fused droplet when the enzymatic reaction is initiated; (b5) Fluorescence image of (b4); (b6) Fluorescence image obtained at reaction time of 25 min. (c) Reaction dynamics curve obtained from the fused droplet in (b4) within 25 min. Scale bar: 100 μm.

Benefiting from the high controllability of the present system on the composition of each droplet, we developed a novel and simple droplet fusion method based on the use of the difference of droplet interfacial tensions. This method does not rely on precise synchronization of sample and reagent droplets, special microchannel geometry, differences between droplet sizes, or any external device with electrical, magnetic, or heating controls, as in the reported droplet fusion systems.[2,30] It only requires that the droplets have different interfacial tensions, which can be easily achieved by varying the compositions of the droplets.

To achieve droplet fusion in a straight and smooth channel, the essential prerequisite is to generate velocity difference between the droplets to be fused. The droplet velocity in a symmetrical circular tube has been characterized as a function of droplet volume, liquid viscosity ratio of droplet to carrier, and capillary number.[31,32] For a series of droplets fully filling the cross section of the channel, their velocities are size independent.[31,32] If there is no evident difference in the viscosity ratios of droplets to carrier, the capillary number will be the main influencing factor on droplet velocity. The capillary number is defined as $Ca = \mu V/\gamma$, where μ is the viscosity of the carrier fluid, V is the bulk velocity, and γ is the interfacial tension between the droplet and carrier phases. In the present system, as the droplet series were suspended in the carrier stream in the capillary channel with the same μ and V values, the velocity differences between these droplets could only be generated by varying the droplet interfacial tension γ.

We first performed droplet fusion experiments with droplets containing different dye solutions with similar viscosities and different interfacial tensions (Table S1, Supporting Information). In Figure 3a1, the yellow, green, and blue dye droplets with interfacial tensions of 0.12, 2.65, and 2.45 mN/m were sequentially aspirated into the capillary channel to form a series of droplet groups. Within one droplet group, the yellow droplet had the lowest interfacial tension among the three dye droplets; thus, it had the highest velocity[31] and could catch up with the green dye droplet during the aspirating process and fused with the latter into one droplet driven by the flow pressure and interfacial force.[8,33] Since the interfacial tension of the fused droplet (0.46 mN/m) was also lower than that of the blue droplet, these two droplets could further fuse with each other. A movie recording these processes is available in the Supporting Information. This droplet fusion method was also feasible for other dye droplets, as shown in Figure 3a2. In addition, the droplet fusion sequence could be flexibly changed by adjusting the oil volume between these three droplets (Figure 3a3). In the above experiments, the droplet fusion was achieved using the natural difference in interfacial tensions of the dye solutions. In real sample analysis, the interfacial tensions of droplets could be adjusted by changing the droplet compositions, e.g., adding surfactant. We also demonstrated the feasibility of this strategy by adding surfactant Tween 20 in the last droplet in a PBS droplet group to achieve sequential fusions of droplets (Figure S4a,b, Supporting Information).

In the intracellular enzyme activity assays performed above, the single cell, lysis reagent, and substrate solutions were mixed during the droplet generation process. The enzyme-catalyzed hydrolysis reaction of FDG took place after the cell lysis and intracellular enzyme release, which usually required 30−120 s. This lag time had no evident effect on long-time measurements. However, for online monitoring of a dynamic process in a short period, an accurate initial point is essential. This could be accomplished in the present system using the droplet fusion method by adjusting the droplet interfacial tensions. We performed a short-term (25 min), accurate monitoring on the initial stage of the enzyme-catalyzed reaction by intracellular β-galactosidase in a single cell. A group of three droplets was first formed in the capillary with a droplet introducing sequence of substrate FDG solution, cell suspension, and lysis reagent (Figure 3b1). The lysis reagent droplet containing surfactants of 0.2% Triton X-100 and 0.2% Tween 20 for cell lysis and adjustment of interfacial tension had the lowest interfacial tension in the droplet group. Under an aspirating rate of 1 nL/s, it could catch up, contact (Figure 3b1), and fuse (Figure 3b2) with the cell suspension droplet within 5 s. After the droplet fusion, the flow in the capillary was stopped for 5 min to ensure the completion of the cell lysis and intracellular enzyme release. Then, the aspiration pump was started up again. Since the fused droplet had relatively low interfacial tension for containing the surfactant components, it could catch up and fuse with the substrate droplet (Figure 3b3,b4). At the moment of this droplet fusion, the monitoring for the enzymatic reaction was started up by recording the droplet fluorescence intensity at 5 min intervals in 25 min (Figure 3b5,b6,c). This droplet fusion method not only achieved the addition of new reagents to the droplets to implement the multistep reactions but also ensured a definite start time of the reaction to be monitored, which is important for the accurate reaction dynamics study.

Solid-Phase Extraction for Single Cell DNA Purification. Solid-phase extraction is a commonly used sample pretreatment technique in routine biological analysis, for example, purification of nucleic acids from cells, which usually requires multiple liquid handling steps including cell lysis, DNA or RNA extraction, washing, and recovering. In most of the droplet-based systems, solid-phase extraction is usually achieved using magnetic beads and magnetic droplet manipulation technique.[17,18,34,35] DNA

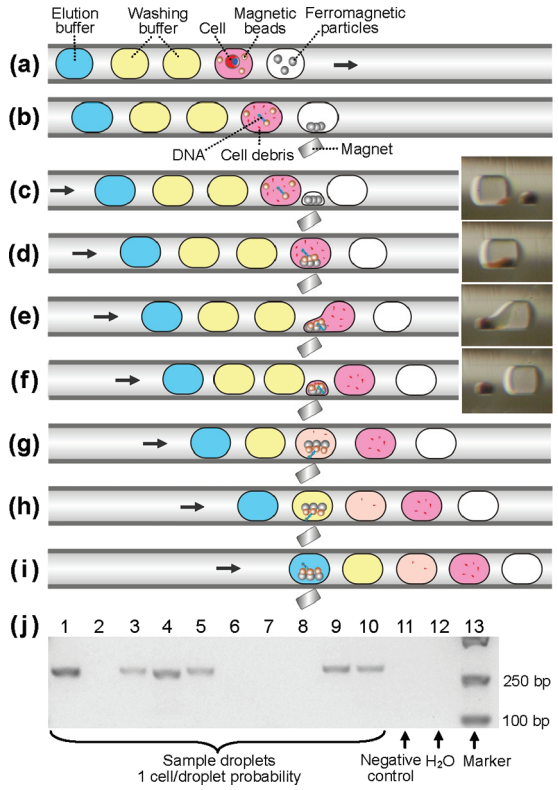

Figure 4. (a–i) Schematic diagram of DNA purification from a single cell: (a) Generation of a series of droplets containing ferromagnetic particles, magnetic beads and cell suspension, washing buffer, and elution buffer. (b) Binding of released DNA to magnetic beads after cell lysis. (b–c) Extraction of ferromagnetic particles. (d) Attraction of DNA–bead complex to ferromagnetic particles. (e–f) Extraction of ferromagnetic particle/DNA–magnetic bead cluster. (g–h) Two washing steps to sufficiently remove interfering cell debris, proteins, and lipids. (i) Recovery of DNA in elution buffer droplet for subsequent PCR amplification. (j) Typical agarose gel electropherogram obtained in the PCR experiment of 38 cycles. Target fragment: 295 bp fragment of human β-actin; line 1–10: 10 sample droplets with an average cell-encapsulation probability of 1 cell/droplet; line 11: negative control; line 12: H_2O; line 13: marker. The arrows represent the flow directions of liquids in the capillary channel.

purification from cells has been demonstrated in an open two-dimensional magnetic droplet manipulation system.[17,34] However, these systems commonly handled droplets in the range of several microliters, which were difficult to be applied in single cell analysis with picoliter-scale droplets frequently used to fit the small cell sizes.[20,21,23,24,26] To the best of our knowledge, so far, there is no report of solid-phase extraction system based on manipulations of picoliter-scale droplets.

When the droplet volumes decrease from microliter or nanoliter to picoliter scale, the droplet interfacial tensions increase dramatically, which significantly increase the difficulty in droplet manipulation. We first performed magnetic-assisted solid-phase extraction in a 10 nL droplet (250 μm i.d. capillary) with 2.8 μm magnetic beads. The beads could be easily separated from the droplet by magnetic force. When the droplet volume was reduced to 500 pL (75 μm i.d. capillary), the magnetic beads (1.5 mg/mL) could not traverse through the oil/water interface to achieve the separation due to the increased droplet interfacial tension. Even increasing the concentration of the magnetic beads by 30-fold to enhance the magnetic force, they still could not pass through the phase interface (see movies in the Supporting Information). Similar phenomena were also reported by other researchers.[18,34,36]

To overcome this difficulty, we developed a simple method by introducing micrometer-scale ferromagnetic particles in the droplet system as carriers to assist the magnetic beads in passing through the phase interface. The ferromagnetic particles, which served as small carrier magnets in the droplet, could directly contact the magnetic beads and attract them into a cluster structure, which increased the magnetic force of the magnet acting on the beads. With this strategy, phase separation between the droplet and the ferromagnetic particle/magnetic bead cluster was successfully achieved in even smaller droplets of 300 pL (see movie in the Supporting Information). Due to the hydrophilic surfaces of the ferromagnetic particles and magnetic beads, the cluster carried a small amount of water with it when separated from the droplet, which exhibited that the droplet was split into a larger droplet and a smaller droplet mainly consisted of the cluster (Figure 4f).

With this breakthrough in phase separation method for picoliter droplet and magnetic beads, we achieved multistep solid-phase extraction among picoliter-scale droplets for the first time and applied the system in DNA purification for single cells. Multiple droplet manipulations including droplet generation, transferring, merging, and splitting were performed, to achieve single cell encapsulation, cell lysis, DNA binding to the magnetic beads, washing, and recovery. The working process is shown schematically in Figure 4. Benefiting from the ability of DropLab in generating droplet array with different compositions, a series of droplets were first generated sequentially in the capillary: 2 nL droplet of ferromagnetic particle solution; 300 pL droplet composed of 100 pL PC12 cell suspension, and 200 pL of magnetic bead solution; two 300 pL droplets of washing buffer; 600 pL droplet of elution buffer (Figure 4a). The droplet array was allowed to stay in the capillary for 5 min to achieve cell lysis and binding of the released DNA to the magnetic bead surface (Figure 4b). Then, the syringe pump was started up again to aspirate the droplet array further into the capillary. When the ferromagnetic particle-containing droplet flowed through the magnetic field region, the ferromagnetic particles were attracted on the side wall of the capillary and separated from the flowing droplet (Figure 4b–c). When the DNA–bead-containing droplet further flowed through the magnetic field region, the DNA–beads were attracted to the ferromagnetic particles forming a cluster of ferromagnetic particles/DNA–magnetic beads, which was separated from the droplet containing cell debris and other cell contents by droplet splitting (Figure 4d–f). Then, the cluster was washed sequentially with two washing buffer droplets to remove any residual contaminants and potential PCR inhibitors (Figure 4g–h). Finally, the elution buffer droplet recovered the ferromagnetic particles and DNA–beads and was pushed out into a PCR tube for subsequent PCR amplification (Figure 4i).

We applied the system in single cell DNA purification from human lung carcinoma (A549) cells. After the DNA purification, fragments with 295-bp from human β-actin genes were amplified and analyzed by agarose gel electrophoresis. Since the cell encapsulated into the droplet was lysed by the cell lysis buffer immediately as the droplet was formed, it was difficult to count the cell number in a droplet clearly using the current setup. In order to demonstrate the feasibility of the present system in

single cell DNA purification for PCR amplification, we carried out the experiments for 5 times, each with 10 sample droplets with an average cell-encapsulation probability of 1 cell/droplet, and compared the experiment results with the cell encapsulation probability experiment at the same conditions. The typical result of a group of 10 sample droplets is shown in Figure 4j, the amplified products were detected in 6 droplets of them, and no signal was detected in the negative control. Among the total 50 sample droplets in the 5 experiments (Figure 4j and Figure S6, Supporting Information), the amplified products were detected in 28 of them, which means that the probability of positive results was ~56%. According to the results of the cell encapsulation probability experiment at the same conditions (Figure 1b), the probabilities of droplets without cells, containing single cell and more than one cell were approximately 36%, 47%, and 17%, respectively. Thus, the positive probability of the single cell DNA amplification experiments was close to the sum probability of 64% for droplets encapsulating a single cell and more than one cell, which implies that the DNA amplifications for most of the single cell droplets were successful. In addition, a comparison experiment without DNA purification by magnetic beads was also performed simultaneously. The procedure of the comparison experiment was similar to that of single cell DNA purification and amplification experiments, except that no magnetic beads were added to the droplets for DNA extraction and purification. No amplified product was detected in 10 sample droplets (Figure S5, Supporting Information), which demonstrated the necessity of DNA purification for single cell DNA amplification in the present conditions.

CONCLUSION

In summary, we have established an automated and multifunctional platform which permits flexible generation and complex manipulation of picoliter-scale droplets and demonstrated its feasibility and potentials in enzyme assay and DNA purification at the single cell level. The platform could be easily built without the need of complicated or expensive microfabrication equipments. As complexity of droplet manipulations increased, the operation of the platform remained convenient and user-friendly by employing a computer program to automatically control the system operation. In this work, two droplet manipulation techniques in picoliter-scale were developed on the basis of the DropLab platform,[29] including sequential droplet fusion based on the interfacial tension difference and magnetic-assisted solid-phase extraction among picoliter-scale droplets. The former technique provided a novel strategy for achieving sequential droplet fusion in droplet-based microfluidic systems, which has advantages of simple system structure, convenient operation, and flexible adjustment to fusion sequence. With the latter technique, we achieved single cell DNA purification based on solid-phase extraction in a droplet-based microfluidic system for the first time. Although the analysis throughput of the present system was relatively lower than those of the continuous-flow droplet systems due to the use of the batch mode, it could achieve complex droplet manipulations that are difficult to perform for the latter systems. In addition, since the present platform was built mainly based on a capillary, its analysis throughput could be further increased using multicapillary array.

The present platform provides a potential alternative to previous droplet-based microfluidic systems for single cell analysis. Furthermore, with the ability of complex multistep droplet manipulations, it may also be applied in multistep biochemical treatment and analysis for small amounts of samples, such as RNA and protein purification, heterogeneous immunoassay (e.g., ELISA), and proteomic assay with mass spectrometric detection at the single cell level.

ASSOCIATED CONTENT

Supporting Information. Additional information as noted in text. This material is available free of charge via the Internet at http://pubs.acs.org.

AUTHOR INFORMATION

Corresponding Author

*E-mail: fangqun@zju.edu.cn.

Present Addresses

†Department of Chemistry, Renmin University of China, Beijing 100872, China.

ACKNOWLEDGMENT

Financial support from National Natural Science Foundation of China (Grants 20775071, 20825517, and 20890020), Ministry of Science and Technology of China (Grants 2007CB714503 and 2007CB914100), and the Fundamental Research Funds for the Central Universities of China are gratefully acknowledged. The authors thank Dr. Yingyan Fan (Department of Pharmacology, Zhejiang University) for providing PC 12 cells and helpful discussion.

REFERENCES

(1) Song, H.; Chen, D. L.; Ismagilov, R. F. *Angew. Chem., Int. Ed.* **2006**, *45*, 7336–7356.
(2) Teh, S. Y.; Lin, R.; Hung, L. H.; Lee, A. P. *Lab Chip* **2008**, *8*, 198–220.
(3) Chiu, D. T.; Lorenz, R. M.; Jeffries, G. D. M. *Anal. Chem.* **2009**, *81*, 5111–5118.
(4) Thorsen, T.; Roberts, R. W.; Arnold, F. H.; Quake, S. R. *Phys. Rev. Lett.* **2001**, *86*, 4163–4166.
(5) Joanicot, M.; Ajdari, A. *Science* **2005**, *309*, 887–888.
(6) Song, H.; Tice, J. D.; Ismagilov, R. F. *Angew. Chem., Int. Ed.* **2003**, *42*, 767–772.
(7) Zheng, B.; Roach, L. S.; Ismagilov, R. F. *J. Am. Chem. Soc.* **2003**, *125*, 11170–11171.
(8) Hung, L. H.; Choi, K. M.; Tseng, W. Y.; Tan, Y. C.; Shea, K. J.; Lee, A. P. *Lab Chip* **2006**, *6*, 174–178.
(9) Lorenz, R. M.; Edgar, J. S.; Jeffries, G. D. M.; Zhao, Y. Q.; McGloin, D.; Chiu, D. T. *Anal. Chem.* **2007**, *79*, 224–228.
(10) Frenz, L.; El Harrak, A.; Pauly, M.; Begin-Colin, S.; Griffiths, A. D.; Baret, J. C. *Angew. Chem., Int. Ed.* **2008**, *47*, 6817–6820.
(11) Adamson, D. N.; Mustafi, D.; Zhang, J. X. J.; Zheng, B.; Ismagilov, R. F. *Lab Chip* **2006**, *6*, 1178–1186.
(12) Nie, J.; Kennedy, R. T. *Anal. Chem.* **2010**, *82*, 7852–7856.
(13) Kiss, M. M.; Ortoleva-Donnelly, L.; Beer, N. R.; Warner, J.; Bailey, C. G.; Colston, B. W.; Rothberg, J. M.; Link, D. R.; Leamon, J. H. *Anal. Chem.* **2008**, *80*, 8975–8981.
(14) Schaerli, Y.; Wootton, R. C.; Robinson, T.; Stein, V.; Dunsby, C.; Neil, M. A. A.; French, P. M. W.; DeMello, A. J.; Abell, C.; Hollfelder, F. *Anal. Chem.* **2009**, *81*, 302–306.
(15) Wheeler, A. R. *Science* **2008**, *322*, 539–540.
(16) Luk, V. N.; Wheeler, A. R. *Anal. Chem.* **2009**, *81*, 4524–4530.
(17) Lehmann, U.; Vandevyver, C.; Parashar, V. K.; Gijs, M. A. M. *Angew. Chem., Int. Ed.* **2006**, *45*, 3062–3067.

(18) Pipper, J.; Inoue, M.; Ng, L. F. P.; Neuzil, P.; Zhang, Y.; Novak, L. *Nat. Med.* **2007**, *13*, 1259–1263.
(19) Sims, C. E.; Allbritton, N. L. *Lab Chip* **2007**, *7*, 423–440.
(20) Koster, S.; Angile, F. E.; Duan, H.; Agresti, J. J.; Wintner, A.; Schmitz, C.; Rowat, A. C.; Merten, C. A.; Pisignano, D.; Griffiths, A. D.; Weitz, D. A. *Lab Chip* **2008**, *8*, 1110–1115.
(21) Clausell-Tormos, J.; Lieber, D.; Baret, J. C.; El-Harrak, A.; Miller, O. J.; Frenz, L.; Blouwolff, J.; Humphry, K. J.; Koster, S.; Duan, H.; Holtze, C.; Weitz, D. A.; Griffiths, A. D.; Merten, C. A. *Chem. Biol.* **2008**, *15*, 427–437.
(22) Chabert, M.; Viovy, J. L.. *Proc. Natl. Acad. Sci. U.S.A.* **2008**, *105*, 3191–3196.
(23) He, M. Y.; Edgar, J. S.; Jeffries, G. D. M.; Lorenz, R. M.; Shelby, J. P.; Chiu, D. T. *Anal. Chem.* **2005**, *77*, 1539–1544.
(24) Shim, J. U.; Olguin, L. F.; Whyte, G.; Scott, D.; Babtie, A.; Abell, C.; Huck, W. T. S.; Hollfelder, F. *J. Am. Chem. Soc.* **2009**, *131*, 15251–15256.
(25) Huebner, A.; Srisa-Art, M.; Holt, D.; Abell, C.; Hollfelder, F.; deMello, A. J.; Edel, J. B. *Chem. Commun.* **2007**, 1218–1220.
(26) Joensson, H. N.; Samuels, M. L.; Brouzes, E. R.; Medkova, M.; Uhlen, M.; Link, D. R.; Andersson-Svahn, H. *Angew. Chem., Int. Ed.* **2009**, *48*, 1–5.
(27) Hong, J. W.; Studer, V.; Hang, G.; Anderson, W. F.; Quake, S. R. *Nat. Biotechnol.* **2004**, *22*, 435–439.
(28) Marcus, J. S.; Anderson, W. F.; Quake, S. R. *Anal. Chem.* **2006**, *78*, 3084–3089.
(29) Du, W. B.; Sun, M.; Gu, S. Q.; Zhu, Y.; Fang, Q. *Anal. Chem.* **2010**, *82*, 9941–9947.
(30) Yang, C. G.; Xu, Z. R.; Wang, J. H. *TrAC, Trends Anal. Chem.* **2010**, *29*, 141–157.
(31) Martinezt, M. J.; Udell, K. S. *J. Fluid. Mech.* **1990**, *210*, 565–591.
(32) Lac, E.; Sherwood, J. D. *J. Fluid. Mech.* **2009**, *640*, 27–54.
(33) Eggers, J.; Lister, J. R.; Stone, H. A. *J. Fluid. Mec.* **1999**, *401*, 293–310.
(34) Pipper, J.; Zhang, Y.; Neuzil, P.; Hsieh, T. M. *Angew. Chem., Int. Ed.* **2008**, *47*, 3900–3904.
(35) Zhang, Y.; Park, S.; Liu, K.; Tsuan, J.; Yang, S.; Wang, T. H. *Lab Chip* **2011**, *11*, 398–406.
(36) Long, Z. C.; Shetty, A. M.; Solomon, M. J.; Larson, R. G. *Lab Chip* **2009**, *9*, 1567–1575.